Journal of Catalysis **193,** 248–254 (2000)
doi:10.1006/jcat.2000.2896, available online at http://www.idealibrary.com on IDEAL®

Fe–MCM-41 as a Catalyst for Sulfur Dioxide Oxidation in Highly Concentrated Gases

A. Wingen,* N. Anastasievič,† A. Hollnagel,† D. Werner,† and F. Schüth*,[1]

**Max-Planck-Institut für Kohlenforschung, Kaiser-Wilhelm-Platz 1, 45470 Mülheim, Germany;*
and †Lurgi Metallurgie GmbH, Lurgiallee 5, 60295 Frankfurt/Main, Germany

Received December 9, 1999; revised March 30, 2000; accepted April 10, 2000

The catalytic properties of Fe–MCM-41 and other iron-based catalyst materials for sulfur dioxide oxidation in highly concentrated gases have been characterized for the first time. Independent of whether the catalysts were synthesized by incipient wetness impregnation, solid-state impregnation, or *in situ* synthesis, the activity is found to be substantially higher than that observed for an industrial iron-on-silica reference catalyst. Although some activity is lost during the formation of the catalysts, Fe–MCM-41 catalysts are remarkably stable at temperatures of up to 1023 K. Fe–MCM-41 catalysts appear to be efficient for the conversion of highly concentrated gases that cannot be processed by conventional vanadium-based catalysts due to thermal breakdown. © 2000 Academic Press

Key Words: **sulfuric acid; catalyst; iron; Fe–MCM–41; sulfur dioxide oxidation; sulfuric acid; mesoporous oxide.**

INTRODUCTION

The oxidation of sulfur dioxide is the basic step in the production of sulfuric acid. Conventionally, vanadium pentoxide catalysts are used. Since BASF was granted a patent for these catalysts in 1913 (1), little effort has been invested in developing alternative catalysts. However, the search for novel catalyst systems has become interesting again from an economical as well as an ecological point of view.

In metallurgical plants copper, zinc, and lead sulfides react with oxygen to form the corresponding metaloxides. Sulfur dioxide is obtained as a by-product and has to be removed from the tail gas for environmental reasons. As environmental legislation becomes more restrictive, this sulfur dioxide accounts for a continuously increasing proportion of the total sulfur dioxide used for sulfuric acid production. In metallurgical plants air is increasingly replaced with oxygen (2), and in such processes the sulfur dioxide content of the tail gas is drastically increased. If it were possible to handle such highly concentrated gases directly, the sulfuric acid plants could be built considerably smaller and would, therefore, be cheaper in construction and operation. In addition, high sulfur dioxide concentrations lead to high temperatures, since the sulfur dioxide oxidation is a strongly exothermic reaction. At high temperatures heat recovery is favored and high-pressure steam could become a valuable by-product. Conventional vanadium-based catalysts, however, are not suitable for handling such high temperatures due to thermal breakdown and loss of vanadium, entailing pollution of the product acid. Furthermore, vanadium-based catalysts require an O_2/SO_2 ratio of about 1.1 to provide high conversions (3). Therefore, the reaction gas from oxygen-based smelter processes needs to be diluted to a greater extent than would otherwise be necessary to maintain the stoichiometric O_2/SO_2 ratio of 0.5. Today tail gases with concentrations of 50% to 70% of sulfur dioxide (Kivcet process) (4) or even 80% (Inco Flash Smelting process) (5) are diluted and processed with a maximum sulfur dioxide concentration of about 8%.

In combination with an indispensable high-temperature stability, low-temperature activity is highly desirable for a new catalyst, since it would increase the range for the adiabatic temperature rise, especially in the first bed. This range is limited, since external cooling becomes necessary as soon as the equilibrium conversion is reached (6).

The active phase of vanadium-based catalysts is a melt under reaction conditions; therefore, the reaction is not surface limited, but the whole volume of the active component is used. In order to obtain comparably active catalysts with solid active phases, high surface areas of the active phase are required.

The discovery of the M41S family of mesoporous silicate and aluminum silicate materials by scientists at Mobil Oil Corp. in 1992 (7) has offered new possibilities to develop active catalysts based on active components other than vanadium. We have used MCM-41, the hexagonally structured member of the M41S family, as a support for iron oxide. MCM-41 exhibits surface areas of about 1000 m^2/g and high thermal stability and should be chemically resistant against the demanding conditions in sulfuric acid plants.

---

[1] To whom correspondence should be addressed. Fax: 49-208-3062995. E-mail: schueth@mpi-muelheim.mpg.de.

0021-9517/00 $35.00

METHODS

The MCM-41 was synthesized in alkaline medium as described by Kresge *et al.* (7). The iron was loaded into the MCM-41 by three different methods. $Fe(NO_3)_3$ was used as the precursor in the case of both incipient wetness and solid-state reaction. For the solid-state loading, the oxide and the iron nitrate were thoroughly ground together, heated at a rate of 5 K/min to 673 K, held at this temperature for 3 h, heated at 5 K/min to 973 K, and maintained at this temperature for 3 h. For *in situ* incorporation, $K_4[Fe(CN)_6]$ was used instead of the nitrate, and was added to the surfactant solution ($C_{16}H_{33}N(CH_3)_3Cl$ in water) before it was combined with the silica solution. The samples were calcined at 973 K to ensure that the temperatures reached during the catalytic experiment did not lead to thermal breakdown of the catalyst.

Structural information was obtained by X-ray diffraction (Stoe, StadiP) using Cu$K\alpha$ radiation. N_2 adsorption experiments were made at 77.35 K (Micromeritics ASAP 2000). Transmission electron microscopy (TEM) was performed with a Hitachi HS2000 (cold field emitter) equipped with an EDAX system (Nora) with an Si(Li) detector. The spatial resolution of the EDAX analysis was about 10 nm. ^{57}Fe Mössbauer experiments (Halder) were carried out at room temperature.

Catalytic sulfur dioxide oxidation was investigated with a gas composed of 20% SO_2, 22% O_2, and 58% N_2. The catalysts were pressed in a manual pellet press to cylindrical pellets, crusted in a mortar, and sieved to obtain the fraction of particles between 500 and 1000 μm. An open flow reactor (i.d. 10 mm) system equipped with nondispersive IR (URAS 3G, Hartmann & Braun) for the sulfur dioxide analysis was used. The catalyst bed height was about 10 mm. The catalyst temperature was measured by a thermocouple placed within a capillary in the catalyst bed. For most experiments a stainless steel system has been used. For reactions at temperatures exceeding 973 K, however, the blank activity of the system was too high ($>5\%$ conversion). These experiments were therefore carried out in a reactor made from fused silica. The sulfur trioxide was removed from the product gas prior to analysis using sulfur trioxide filters (Fuhr) and the offgas was only passed through the IR cell during analysis. For the investigation of the temperature dependence of the conversion, each temperature was held constant for 2 h before the conversion was determined and the temperature was raised. Although this particular time period might not be sufficient to fully reach steady-state conditions in all cases, it was regarded as suitable for comparison of different catalysts.

RESULTS AND DISCUSSION

For incipient wetness impregnation utilizing $Fe(NO_3)_3$ as the iron precursor the Si : Fe ratio was varied in the range of Si : Fe = 100 : 1 to Si : Fe = 5 : 1. With increasing iron content, samples show a decrease in both mesopore volume and BET surface area, even if the additional weight of iron oxide deposited is considered as not contributing to the surface area and is therefore neglected when normalizing surface area to weight. The decrease may be caused by pore blockage. The BET surface area decreases less than the mesopore volume. This is because the total surface area is the sum of internal and external surface area, and only the internal surface is influenced by the loading. However, the full pore volume is affected by the introduction of the iron. While many samples have been evaluated catalytically, only selected results typical for each class of materials are shown. For the sample for which catalytic results are shown below, the MCM-41 support material had a BET surface area of 775 m^2/g before impregnation and a BET surface area of 530 m^2/g after impregnation with Si : Fe = 5 : 1 and calcination at 973 K.

For *in situ* synthesis, $K_4[Fe(CN)_6]$ turned out to be a highly suitable iron precursor. Previous studies carried out in our laboratory led to the conclusion that the synthesis of pure silica MCM-41—if fumed silica is used as silica source—is highly sensitive to slight changes in the synthesis procedure such as using magnetic stir bars of different sizes (8). The addition of $K_4[Fe(CN)_6]$ to the synthesis mixture, however, seems to promote the reproducibility of the synthesis of a material with several sharp, well-defined XRD low-angle reflections. For Si : Fe ratios in the range of Si : Fe = 20 : 1 to Si : Fe = 35 : 1 highly ordered materials with high mesopore volume, sharp pore size distribution, and high BET surface areas can be obtained. Increasing or decreasing the iron content leads to materials for which the features described above appear to be less pronounced. The sample for which catalytic results are shown below was synthesized with Si : Fe = 20 : 1 and calcined at 973 K. In transmission electron microscopy this sample appears to be hexagonally ordered throughout almost the whole sample, in contrast to samples which were synthesized via an identical procedure, but without the iron salt. In the case of pure silica MCM-41, hexagonally ordered areas seem to be more rare and ordered only over shorter length scales. In addition, most of the TEM pictures presented in the literature show materials calcined only at 823 K. After calcination at 973 K, pure silica MCM-41 materials sometimes exhibit partially destroyed structures, which was not observed for the sample synthesized in the presence of $K_4[Fe(CN)_6]$. The X-ray diffractogram of this sample shows four well-resolved peaks, which can be indexed hexagonally. The nitrogen sorption isotherm shows a steep increase in the volume adsorbed in the range of relative pressures which is typical for condensation in the mesopores; the surface area is 940 m^2/g. The Si : Fe ratio obtained for this sample was 26 : 1, as measured by EDAX analysis in the TEM.

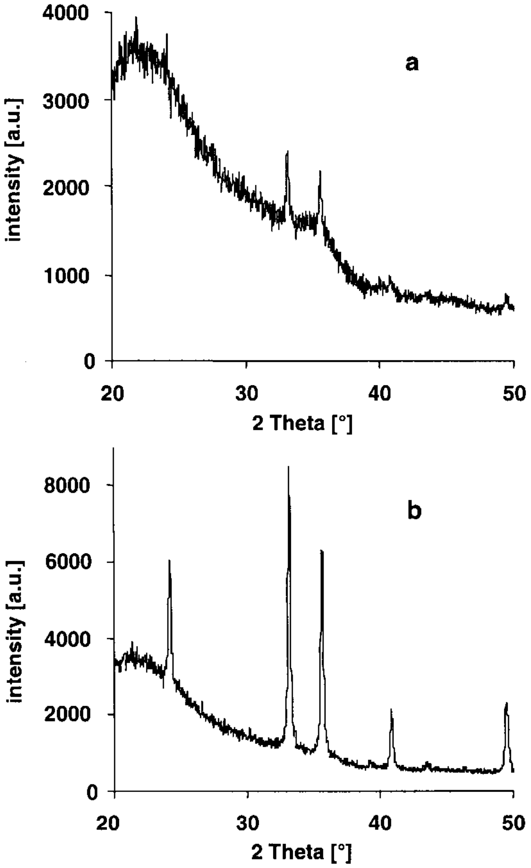

FIG. 1. X-ray diffractograms for samples synthesized by the incipient wetness technique (a) and by solid-state impregnation (b).

The samples obtained via solid-state reaction had an almost unchanged diffraction pattern in the low-angle range. The reflections of the iron nitrate precursor, however, had vanished after the heating step at 973 K; instead, reflections for hematite appeared which were broadened due to particle size effects. Surface areas were reduced to approximately the same extent as for the samples prepared by incipient wetness impregnation, which is also in this case probably due to pore blocking by the iron species.

In order to investigate the state of the iron compound, X-ray diffractograms of samples from the three synthesis pathways were recorded. Figure 1 shows the traces for samples prepared via incipient wetness and solid-state reaction prior to catalytic experiments. For the sample obtained via *in situ* synthesis no iron phase could be detected via X-ray diffraction; the diffraction pattern was featureless in the wide-angle range. For both samples in Fig. 1 the observed reflections can be assigned to Fe_2O_3 (hematite). In the case of the sample impregnated by the incipient wetness technique, the peaks are of low intensity and a strong broadening underlying the sharp reflections indicates an at least bimodal distribution of particle sizes. The line width in the case of the sample prepared by the solid-state impregnation technique allows calculation of the crystallite diameter using the Scherrer formula (9). The calculated particle size is 43 nm. However, due to the relatively low intensities of the hematite reflections it could be concluded that only a fraction of the iron was present in the form of particles detectable via XRD. In order to obtain more information about possible X-ray amorphous particles we carried out additional experiments using Mössbauer spectroscopy. In Fig. 2 the spectra of the samples impregnated by the incipient wetness technique and by solid-state impregnation are shown. The observed sextets are typical for ferromagnetic hematite, and, as expected from the intensities of the peaks in the X-ray diffraction experiment, also here the intensity of the sextet is much stronger for the sample prepared by the solid phase impregnation technique. In addition to the sextets, several other lines are observed. These lines can be fitted by doublets, with isomeric shifts and quadrupole splitting constants typical for a distribution of superparamagnetic hematite (10). Transition from ferromagnetic to superparamagnetic behavior occurs with decreasing particle size, since the time evolution of the magnetization vector is short compared to the time scale of the experiment. Therefore, there is no effective magnetic field at the nucleus on the Mössbauer time scale. For surface atoms, the quadrupole splitting constant is increased due

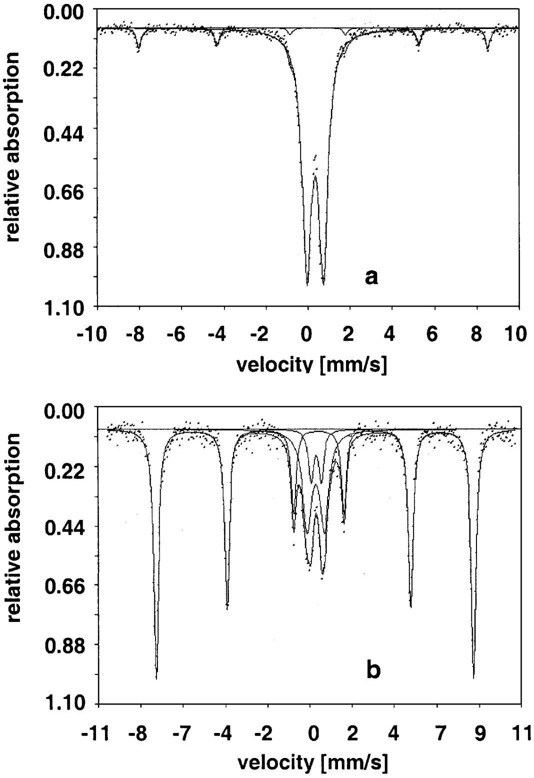

FIG. 2. Mössbauer spectra for samples synthesized by the incipient wetness technique (a) and by solid-state impregnation (b).

to their asymmetric environment. Hence, the magnitude of the quadrupolar splitting allows estimation of particle sizes (10) for particles not detectable by X-ray diffraction. For the sample synthesized by the incipient wetness technique, a particle size of 2.9 nm was obtained; in the case of the sample synthesized by solid-state impregnation, a bimodal distribution with particle sizes of 2.3 and 10.0 nm was calculated. The spectrum of the *in situ* prepared sample only showed a doublet which could be fitted by two different particle sizes of 1.5 and 4.4 nm. However, since the fitting of the doublets remains somewhat ambiguous, the numerical values should be considered as only an estimation of the particle sizes. Moreover, since it is probable that a distribution of particle sizes is present, fitting by many lines would be more appropriate. However, the data quality is not sufficiently good to fit a distribution. The values for the smaller particles, below about 4 nm, suggest that these are species which are located within the MCM-41 channel system. On average, the iron dispersion seems to be lower for the samples prepared by the solid-state reaction, which could be the reason for the lower catalytic activity (see below). There was no indication for iron species present in the freshly prepared catalysts other than the hematite particles of different sizes.

Catalytic experiments were carried out for many different samples with consistent behavior for each mode of preparation. In addition to the samples mentioned above, two industrial catalysts were used as references: a vanadium-based commercial catalyst for sulfur dioxide oxidation (BASF V4-111) and an iron-on-silica catalyst, Si : Fe = 23 : 1 (BASF V1605). In the following the discussion will focus on selected samples which are prototypic for all samples of the series. In Fig. 3 the conversion of sulfur dioxide as a function of temperature is shown, measured at a gas hourly space velocity of 3000 h^{-1}. The Si/Fe ratio of the V1605 catalyst was higher than those for the materials based on MCM-41. In order to check whether this would strongly influence catalytic performance, the iron content was also increased to 5 : 1 by solid-state loading with iron nitrate. The effect on the conversion achieved, however, was small (shifts of <10 K in the conversion curves). Many curves similar to those shown in Fig. 3 have been recorded for different catalyst batches with comparable results. In the following, the typical observations will be discussed for one particular set of materials.

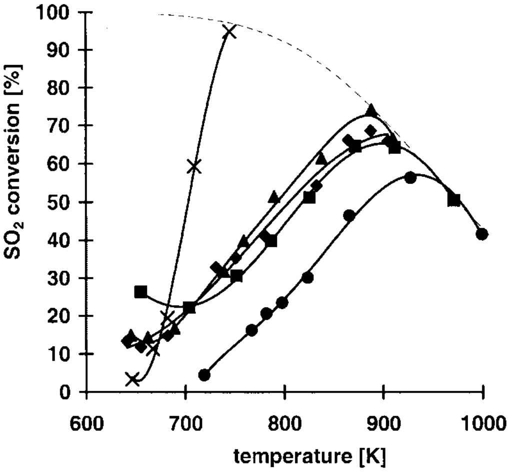

FIG. 3. SO_2 conversion vs T: ▲, incipient wetness impregnation; ◆, solid-state impregnation: ■, *in situ* synthesis; ●, V1605 Fe reference; ×, V4-111 V reference. The connecting lines are just a guide for the eyes. The dotted line shows the equilibrium conversion.

As expected, the low-temperature activity of the MCM-41-based catalysts is considerably lower than that of the vanadium-based catalyst. However, it is substantially higher than that of the iron-based reference catalyst. The differences in the catalytic activities of the Fe–MCM-41 catalysts prepared by the different pathways are small but significant. Considering the rather low iron content, the activity of the sample obtained by *in situ* synthesis is remarkably high. However, materials synthesized with increased iron content showed decreased long-range order and decreased mesopore volume, as described above. The conversions achieved over such catalysts were lower than those for the samples impregnated by postsynthesis methods. In addition, incipient wetness impregnation and solid-phase impregnation are favorable from the industrial point of view, since the support material is in principle commercially available and the loading methods can easily be scaled up. Therefore, further investigations were focussed on materials obtained by postsynthesis loading with iron.

The conversion achieved for the sample impregnated by the incipient wetness technique was slightly higher than that for the one obtained by solid-phase impregnation. This difference, which was not very pronounced, but was consistently observed for many different catalyst batches, might be due to the higher dispersion of the iron species. When conversion versus temperature curves were recorded a second time, significant changes could be observed for all iron-based catalysts. As can be seen in Fig. 4, the activity decreased in the second cycle, resulting in a shift of the conversion curve to approximately 50 K higher temperatures. The extent of the decrease was equal for all three different kinds of Fe-MCM-41 materials examined as well as for the iron reference catalyst. However, the period of time the catalyst was held at 973 K does not influence the degree of deactivation, as investigated for the sample impregnated by the incipient wetness technique in the range of 1 to 90 h. Moreover, in a third cycle the same activities were observed as in the second cycle, indicating that no further short-term deactivation took place under the given reaction conditions. It thus seems more appropriate to describe this initial period over which the activity loss occurs as a formation period.

The catalysts used usually do not show more than two low-angle peaks of relatively low intensity in the X-ray

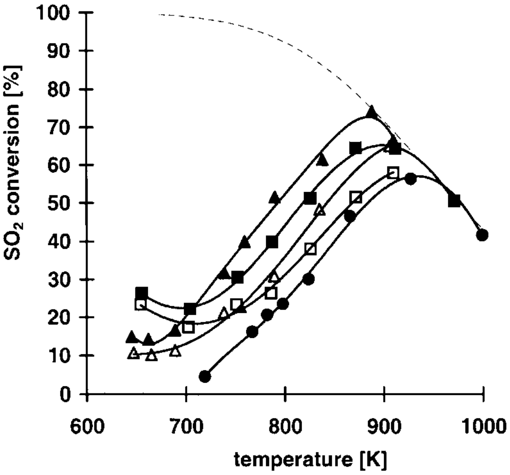

FIG. 4. SO_2 conversion vs T in two consecutive catalytic cycles, incipient wetness impregnation in first (▲) and second (△) cycles, *in situ* synthesis in first (■) and second (□) cycles, V1605 Fe reference (first cycle, ●). The connecting lines are just a guide for the eyes. The dotted line shows the equilibrium conversion.

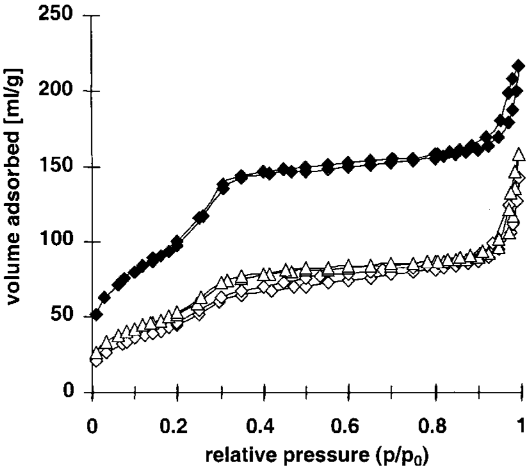

FIG. 6. N_2 sorption isotherms for solid-state impregnated samples before catalysis (◆) and after interruption of the catalytic experiment in the first (◇) and second (△) cycles.

diffraction experiment, and both mesopore volumes and BET surface areas are strongly decreased (by about a factor of 3, see Fig. 6). The loss of structural integrity does not take place for the pure silica MCM-41 support under the given reaction conditions, though. As expected for a silica material, the pure silica parent MCM-41 did not show any change in its properties after being held in an equilibrated reaction gas mixture at 973 K for 12 h. Therefore, this degradation of the support structure must be related to the active iron phase. In order to elucidate whether structural collapse can be responsible for the initial deactivation, the catalytic reaction was interrupted at an identical temperature for one catalyst in the first and for another one only in the second cycle, as shown in Fig. 5 for the sample impregnated by the solid-phase impregnation technique with Si : Fe = 5 : 1. N_2 sorption measurements revealed that the total decrease in mesopore volume and BET surface area could already be observed after interruption in the first cycle without the corresponding decrease in catalytic activity. The isotherms are shown in Fig. 6; the BET surface area decreased from 360 m^2/g before catalysis to 170 m^2/g after interruption in the first cycle and 190 m^2/g after termination of the experiment in the second cycle. Obviously, structural collapse is not responsible for the initial decrease in catalytic activity, since the catalysts obtained in the first catalytic cycle already show structural collapse.

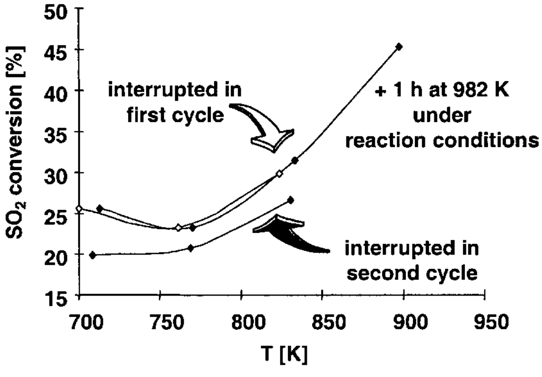

FIG. 5. Interruption of the catalytic experiment in one of two consecutive cycles. The connecting lines are just a guide for the eyes.

Comparison of the crystallite sizes of the iron species observed by peak broadening of the hematite reflections in X-ray diffraction experiments did not show a decrease in dispersion of the hematite species that could be responsible for the observed decrease in activity between the first and the second cycles. Energy dispersive analysis of X rays coupled to transmission electron microscopy was carried out to determine the iron and silicon contents at spots 10 nm in size. At almost all spots iron was detected, indicating a highly dispersed iron species in addition to crystallites detected by X-ray diffraction. However, no clear difference in Si : Fe ratios or their standard distribution could be detected for samples obtained after breaking off the catalysis during the first or second cycle.

However, during the catalytic reaction part of the hematite is converted to an iron sulfate species, as detected in XRD analysis of the used catalysts. The phase distributions for samples removed in the first and the second cycles are slightly, but consistently and reproducibly different. In Fig. 7 the X-ray diffractograms are shown for materials synthesized by the solid-state impregnation technique and incipient wetness impregnation. Two phases are observed in the used samples, $Fe_2(SO_4)_3$ and Fe_2O_3 (hematite). Although the intensity of the $Fe_2(SO_4)_3$ peaks is always much higher than that of the Fe_2O_3 peaks, the $Fe_2O_3/Fe_2(SO_4)_3$ ratio is slightly increased after interruption in the second cycle. This might indicate that part of a highly dispersed and

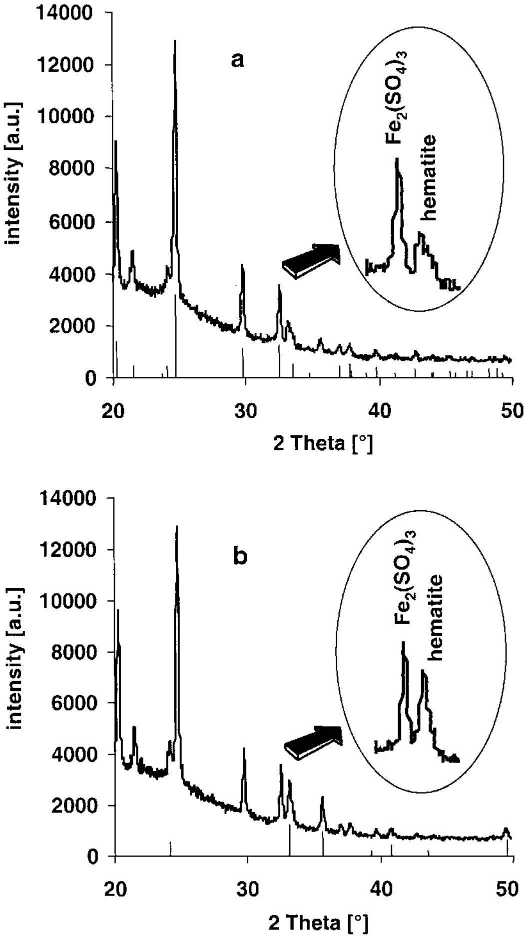

FIG. 7. X-ray diffractograms for solid-state impregnated samples after interruption of the catalytic experiment in the first (a) and second (b) cycles. The reference diffractograms displayed represent $Fe_2(SO_4)_3$ (a) and hematite (b).

active iron species, which forms sulfate under reaction conditions, is converted to less active hematite under catalytic conditions relatively rapidly. It would be tempting to speculate that these are iron species not located in the MCM-41 pore system. However, at present we do not have experimental evidence for this. It must also be mentioned that the X-ray diffraction experiments were carried out in air at room temperature after cooling the catalysts down from reaction temperature in a stream of nitrogen. During this procedure, new species may be formed while others may disappear. Investigations utilizing *in situ* X-ray diffraction would be needed to further substantiate this interpretation. However, due to the corrosive nature of the gases and the problem of SO_3 condensation, such experiments have not been possible so far.

An industrial sulfuric acid catalyst has a service time of several years. From an industrial point of view it is of great importance to obtain information about the loss of activity during prolonged exposure to reaction conditions. A laboratory study cannot fully address this problem; however, deactivation studies were performed over several weeks. Figure 8 shows the activity for a sample impregnated by the solid-state impregnation method and for the iron reference catalyst as a function of the time the catalysts were kept under reaction conditions at 961 and 966 K, respectively. The amount of catalyst was chosen in each case to reach conversions below the equilibrium conversion, because deactivation might go unnoticed under conditions where the conversion reaches equilibrium. (Note the difference in the time scale between Figs. 8a and 8b.) The activity of the solid-state impregnated sample (Fig. 8a) decreases much more slowly than that of the iron reference catalyst (Fig. 8b). Since it was rather difficult to maintain this kind of experiment running for a longer period of time due to the availability of the reaction system for such experiments,

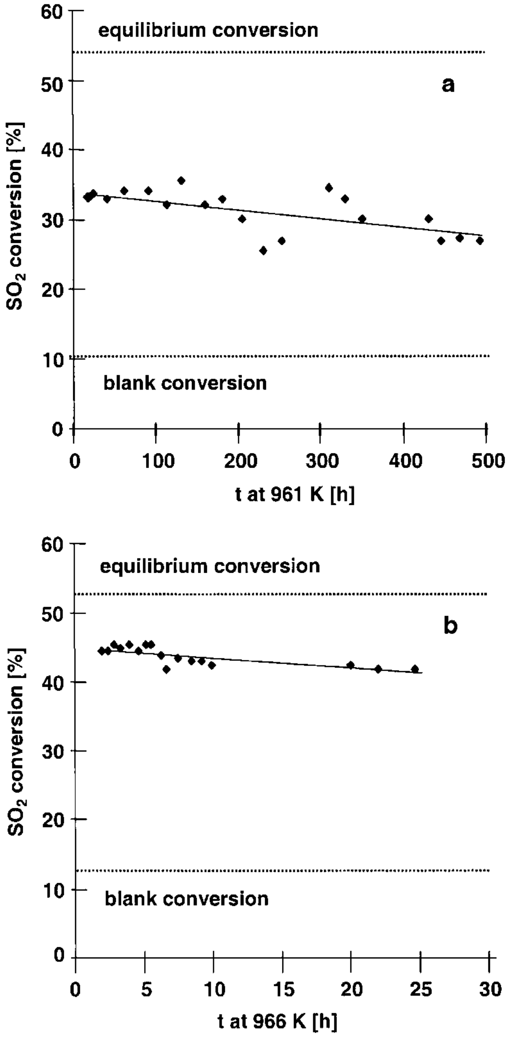

FIG. 8. SO_2 conversion vs time at elevated temperature for the solid-state impregnated sample (a) and the iron reference catalyst (b). Note the difference in the time scales. The dotted line shows the equilibrium conversion.

catalysts were also brought into a quartz tube purged by a reaction gas mixture which had been equilibrated at 1023 K over a catalyst placed before this quartz tube. The quartz tube was closed at both ends at 1023 K and kept at this temperature for 67 days to simulate long-term experiments at this temperature.

After this treatment, the conversion obtained over the catalysts was measured as a function of temperature. The data obtained following this procedure are not very precise, since the amount of catalyst which could be kept in the quartz tubes is too small for a very reliable catalytic test under flow conditions. However, the conversion versus temperature curve was not shifted by more than about 50 K to higher temperatures compared to the catalysts after the formation period, which corresponds to a loss of activity by a factor of about 2 after this harsh treatment. The reason for the long-term deactivation could not be elucidated thus far; no single analytical technique revealed pronounced differences between catalysts after the formation stage and aged catalysts. The deactivation might be the result of a combination of several factors.

Additional long-term experiments at higher temperatures up to 1023 K were carried out under flow conditions at Lurgi AG and showed results comparable to the ones presented in Fig. 8. This deactivation behavior of the catalysts was sufficiently promising such that a pilot plant was installed in a bypass stream of an industrial smelter and has been in operation successfully over several months.

In summary, iron-based catalysts, especially those based on high surface area silica, can be used for the sulfur dioxide oxidation in highly concentrated gases. Catalysts with MCM-41 or similar materials as supports were superior to conventional catalysts based on precipitated silica and show activity versus temperature curves which are shifted to about 50 K lower temperatures. All iron-based catalysts studied show some deactivation during the formation period. This deactivation was also observed for the reference catalyst and is probably due to a change in the phase composition whereby more iron is incorporated in hematite particles. Samples prepared by the incipient wetness technique and held at 1023 K for 67 days still show higher catalytic activity than the iron reference catalyst after the formation period. Therefore, these catalysts seem to be very well suited for the economically and ecologically advantageous oxidation of sulfur dioxide in highly concentrated gases.

ACKNOWLEDGMENTS

The financial support of Lurgi Metallurgie GmbH is gratefully acknowledged. Part of this work was carried out at the University of Frankfurt, the support of which is gratefully acknowledged as well. We thank B. Spliethoff and A. Kornowski for the TEM analyses and K. Kömpe and E. Kühl (Hamburg) for the Mössbauer experiments.

REFERENCES

1. Badische Anilin- & Soda-Fabrik, German patent 291792, 1913.
2. Queneau, P. E., *Metal. Trans.* **8**, 357 (1977).
3. Adlkofer, J., Diekmann, E., and Winkler, E., *Sulfur* **229**, 50 (1993).
4. Chaudhuri, K. B., Koch, M., Paschen, P., and Patino, J. L., *Erzmetall* **32**(7–8), 330 (1979).
5. Merla, S., Young, C. E., and Matousek, J. W., “Environ. Contr., Proc. Symp.” (C. Rampacek, Ed.), pp. 19–35, AIME, New York, 1972.
6. A review on sulfuric acid production is given in the following: Adlkofer, J., *in* “Handbook of Heterogeneous Catalysis” (G. Ertl, H. Knözinger, and J. Weitkamp, Eds.), Vol. 4. VCH, Weinheim, 1997.
7. Kresge, C. T., Leonowicz, M. E., Roth, W. J., and Vartuli, J. S., *Nature* **359**, 710 (1992).
8. Thieme, M., Disser, S., Junges, U., Schacht, S., Schmidt, W., Schüth, F., and Wingen, A., COPS-V, 5th International Symposium on the Characterisation of Porous Solids, Heidelberg, May 30–June 2, 1999.
9. West, A. R., “Solid State Chemistry and its Application.” Wiley, New York, 1984.
10. Kuendig, W., Boemmel, H., Constabaris, G., and Lindquist, R. H., *Phys. Rev.* **142**, 327 (1966).